201967: gold specks in quartz, Middle Creek prospect

(Mosquito Creek Formation, Pilbara Craton)

Sample type	Vein quartz with specks of gold
Total weight	NA
Sample location	Middle Creek prospect, about 8.3 km east-northeast of Nullagine
Coordinates	MGA zone 51, 209328E 7579166N
Datum	GDA94
1:250 000 map sheet	NULLAGINE (SF 51-5)
1:100 000 map sheet	NULLAGINE (2954)
Tenement	P 46/1907
Collector	Blackstone Minerals

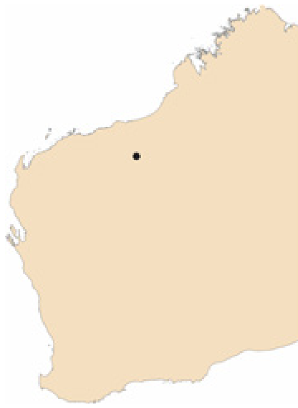

Location and sampling

The sample was provided by Blackstone Minerals in October 2018. It was collected at the Middle Creek prospect in the east Pilbara region (Blackstone Minerals, 2018, written comm., 12 October).

Geological context

The Middle Creek prospect is located in the central part of the Mosquito Creek Basin: a rift basin formed between the East Pilbara and the Kurrana Terranes (Hickman, 2021) about 2 km southeast of the major east-northeasterly striking Blue Spec Fault Zone. The prospect is located between Nullagine and the Blue Spec Au–Sb deposit. It sits within the Nullagine Blue Spec mineralized corridor that hosts numerous gold and gold–antimony deposits in the 2980–2905 Ma Mosquito Creek Formation (Bagas, 2005), along several large east-northeast-striking shear zones and thrust faults (GSWA, 2014). Of these, the Blue Spec deposit has been the most productive, with almost 2 t of gold and concentrates containing 1500 t of antimony (Ferguson and Ruddock, 2001). The mineralization in the Blue Spec deposit is concentrated along the margins of the shear zone, in lodes within quartz veins containing stibnite, aurostibnite, native gold, pyrite, pyrrhotite and carbonate, with minor scheelite, arsenopyrite, marcasite, sphalerite, chalcopyrite, magnetite, calaverite, mackinawite, rickardite, gudmundite, and cervantite in the oxidized zone, and traces of mercury (Hickman, 1983).

The sample was derived from a quartz vein in the Mosquito Creek Formation, which comprises a thick succession of conglomerate, sandstone and shale, most of which was deposited as turbidites in the deepwater trough of the Mosquito Creek Basin (Hickman, 2022). Interlayered psammitic and pelitic metasedimentary rocks with graded bedding and local cross-bedding are the dominant rocks in the Mosquito Creek belt, a fault-imbricated Archean succession of turbiditic metasedimentary rocks and minor mafic–ultramafic metavolcanic rocks (Blackstone Minerals, 2018, written comm., 12 October).

The nearest regolith landform is a colluvial unit comprising unconsolidated colluvial sand, silt, and gravel in outwash fans, scree and talus, and proximal mass-wasting deposits (GSWA, 2014).

Methodology

The sample was photographed and weighed, its morphology and external features, such as colour, roundness, surface relief, coatings, mineral inclusions and mineralogical assemblages, were recorded using visual morphometry. A small subsample containing a gold grain was cut from the main specimen and analysed by using scanning electron microscopy with energy dispersive X-ray spectroscopy (SEM-EDS). The subsample was mounted in epoxy resin and polished to expose gold microstructure and inclusions for examination using reflected-light microscopy and SEM-EDS. Gold microchemistry was determined by laser ablation inductively coupled plasma mass spectrometry (LA-ICP-MS), calibrated against certified gold reference materials (CRM; Murray, 2009). The sample was ablated in duplicate along 0.5 mm-long traverses and average values calculated for elements present in the CRM. The gold surface was repolished after laser ablation, etched with aqua regia, and the internal structure examined using reflected-light microscopy. Details of this method are described in Hancock and Beardsmore (2020).

Morphology

The sample is a fragment of vein quartz containing specks of native gold on an oxidized surface, associated with abundant subhedral goethite grains up to 1 mm in size (Fig. 1a). A grey chlorite–clay veinlet crosscuts quartz and carbonate on the side of the specimen opposite the gold-bearing surface (Fig. 1b).

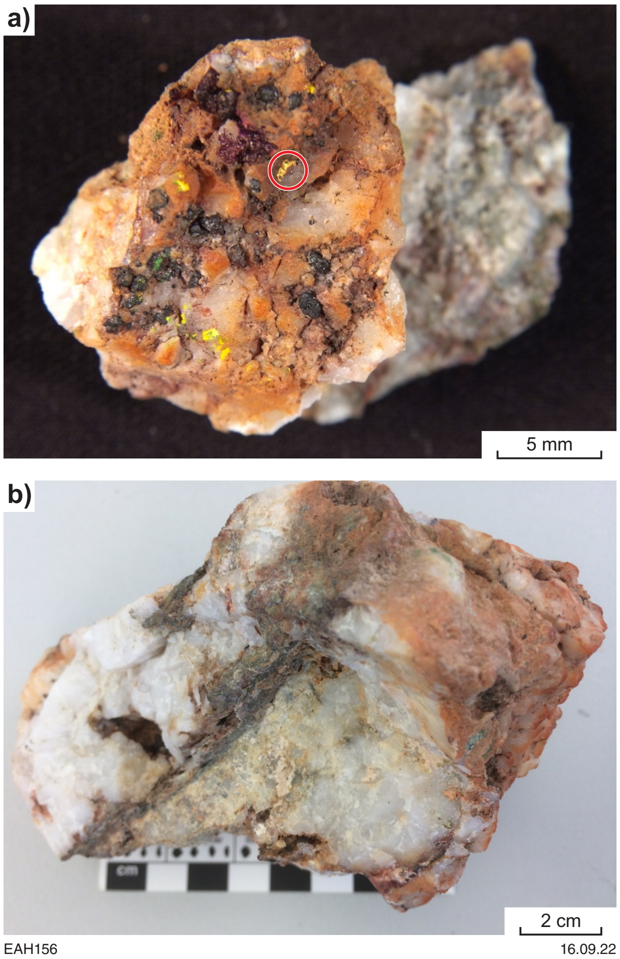

Figure 1. **Sample 201967: gold specks in quartz, Middle Creek prospect: a) oxidized surface with goethite and gold grain (in red circle); yellow–green paint is artificial, and was used to show the location of visible gold in hand specimen; b) opposite side showing chlorite–clay veinlet**

SEM-EDS analysis of raw surfaces

One slightly rounded, irregularly shaped 1.0 × 0.5 mm gold grain occurs in a fissure in quartz (Fig. 2a). The right-hand part of the grain located at the edge of the fissure is more rounded with a more strongly pitted surface and lacks a rim of gold nanoparticles. Gold on smooth surfaces contains 3.5% Ag, whereas gold on pitted surfaces contains no Ag. Nanoparticles of pure gold form a discontinuous, spongy lacework on the surface of the gold grain and occur in Si–Al–(Fe, Mg) clays filling relatively large cavities in the grain (Fig. 2b). Less abundant gold nanoparticles also occur distal to the gold grain, disseminated in quartz–clay mixtures containing Fe, Mg, Ca, K and Ti. Botryoidal goethite has pseudomorphed a pyrite crystal (Fig. 2c), and spherules of organic matter occur within Fe-oxide patches on the weathered surface of quartz (Fig. 2d).

Optical microscopy of polished surfaces

The gold grain is located in a clay-filled fissure in the vein quartz. The grain has an uneven shape and an irregular or scalloped margin suggesting dissolution. Laces of nanoparticles observed on the raw surface are not present on the polished surface. Other small gold particles are dispersed in the clay. Subhedral to rounded pyrite crystals up to 0.5 mm in diameter are heavily oxidized and partly replaced by goethite (Fig. 3a). There is also a small (30 µm), unaltered, euhedral galena crystal in the quartz matrix (Fig. 3b).

SEM-EDS analysis of polished surfaces

The central part of the gold grain contains 10% Ag, whereas there is only 2.3% Ag in the outer rim.

LA-ICP-MS analysis

Analyses consistently detected Ag, Cu and Hg within the gold grains, in concentrations higher than the instrumental detection limit, and probably occurring as limited solid solutions in the gold. Other trace elements were detected only sporadically in low (sub-ppm) concentrations, possibly occurring in micro- and nano-inclusions.

The gold grain contains variable, relatively high Ag (9.3 – 12.0%), low Cu (197–231 ppm), and variable Hg (Table 1). In addition, small concentrations of Pd and Sb were consistently detected in the sample and only traces of Mg (Table 2). The presence of Sb probably reflects the local geochemical environment (known gold–antimony mineralization).

Acid etching

Etching of the surface of the gold grain revealed a polycrystalline internal fabric and a granulated, recrystallized rim up to 200 µm wide along boundaries, mainly in contact with quartz (Fig. 4). Large pits in the gold grain are filled with Fe-oxide minerals, quartz and clays.

Interpretation

Gold in this sample occurs in a clay–chlorite matrix within a fissure in vein quartz. The large grain has an irregular, polycrystalline structure, and contains relatively high Ag and traces of Cu, Hg, Pd and Sb. These characteristics indicate its primary nature and precipitation from low-temperature hydrothermal fluids.

The outer rim of the grain has experienced post-depositional mechanical deformation and recrystallization, and partial chemical dissolution and removal of Ag. Spongy masses of nanoparticles that mantle the surface of the gold grain were possibly introduced by oxidized groundwater, or formed by local dissolution and reprecipitation of gold in the outer high-purity rim of the main grain.

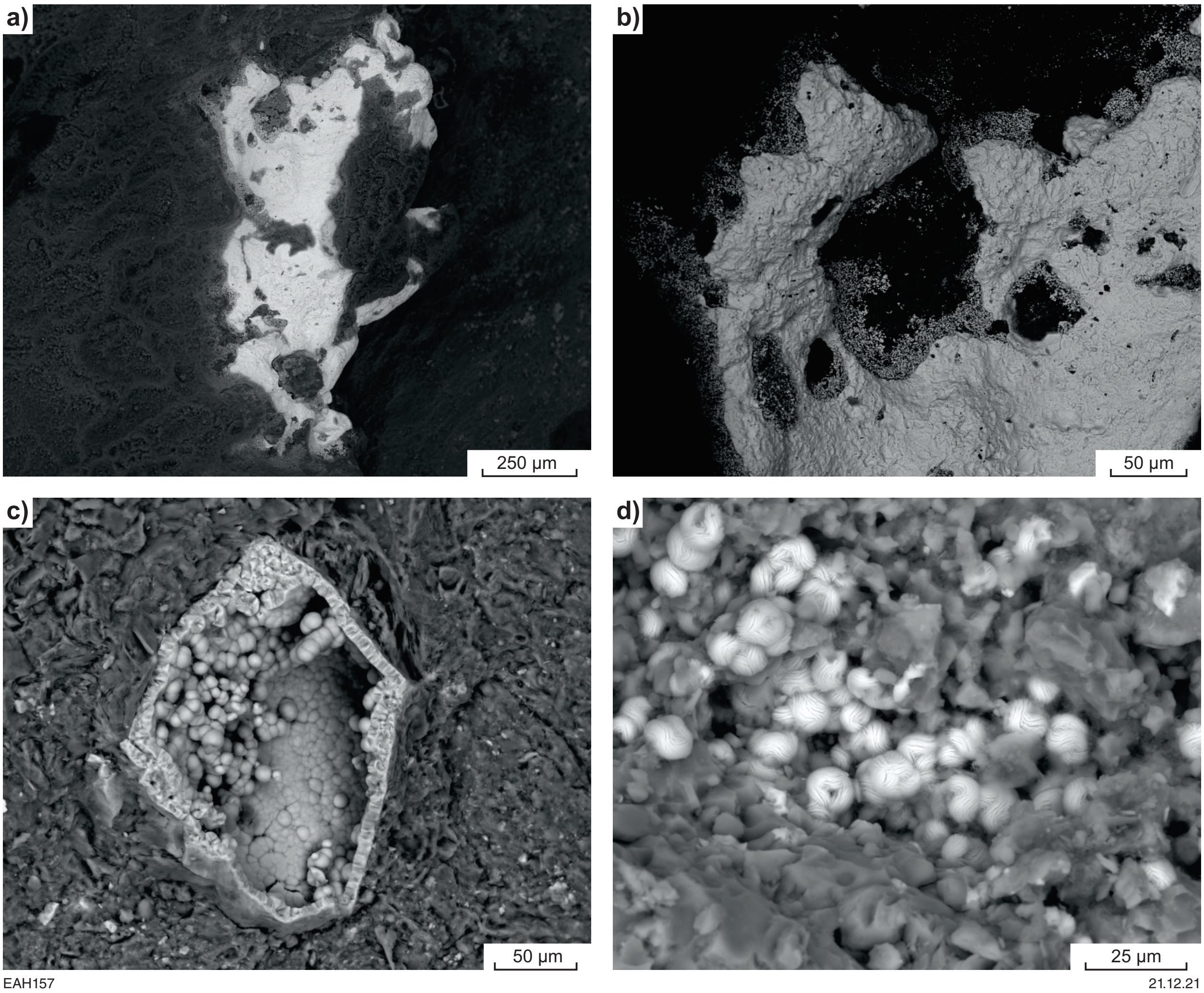

Figure 2. **Backscattered electron (BSE) images (a–c) and secondary electron image (d) of sample 201967: gold specks in quartz, Middle Creek prospect**

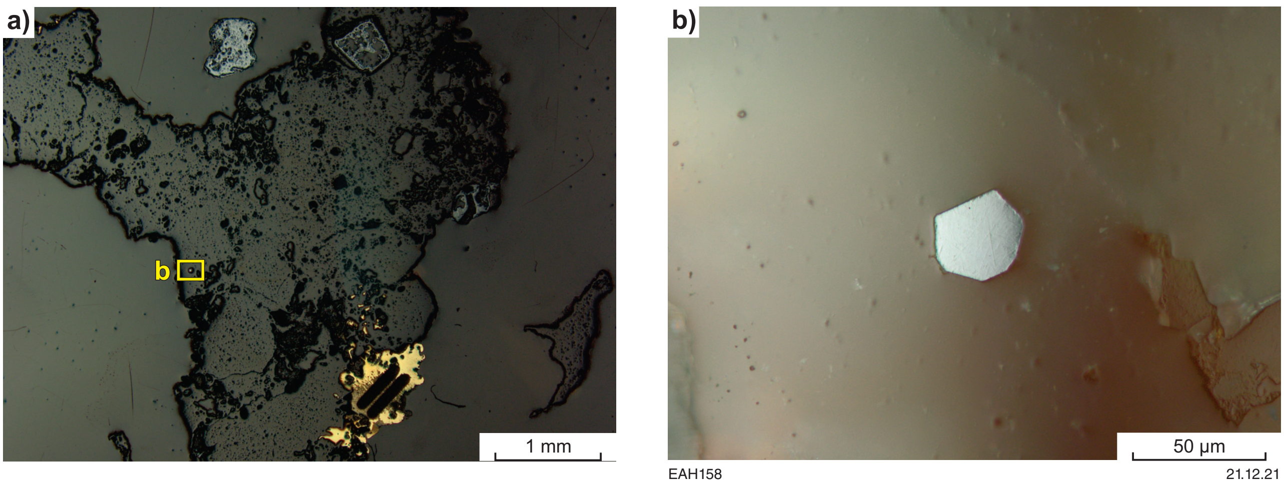

Figure 3. **Reflected-light photomicrographs of polished surface of sample 201967, Middle Creek prospect: a) gold grain and specks in quartz-chlorite matrix with oxidized pyrite crystals. Yellow square shows location of b); b) euhedral galena crystal in quartz matrix. Dark elongate lines in the gold grain are laser ablation tracks produced during LA-ICP-MS analyses**

Table 1. LA-ICP-MS data for selected elements in sample 201967: gold specks in quartz, Middle Creek prospect

Ag (%)	*Cu (ppm)*	*Hg (ppm)*	*Minor elements (ppm)*
9.3, 12.0	197, 231	291, 410	Mg; Pd (3, 3); Sb (2, 5)

Table 2. LA-ICP-MS compositional data for sample 201967: gold specks in quartz, Middle Creek prospect

Laser ablation track	*Unit*	^{7}*Li*	^{9}*Be*	^{11}*B*	^{23}*Na*	^{25}*Mg*	^{27}*Al*	^{29}*Si*	^{44}*Ca*	^{45}*Sc*	^{49}*Ti*	^{51}*V*	^{53}*Cr*	^{55}*Mn*	^{57}*Fe*	^{59}*Co*	^{60}*Ni*	^{65}*Cu*
1	cps					68	6922			15	7	8					5	24426
2	cps					144	1790				5	6	1			8	4	28568
1	ppm					0.81					0.14						0.05	197.30
2	ppm					1.72					0.10						0.04	230.76

Laser ablation track	*Unit*	^{66}*Zn*	^{69}*Ga*	^{72}*Ge*	^{75}*As*	^{82}*Se*	^{85}*Rb*	^{88}*Sr*	^{89}*Y*	^{90}*Zr*	^{93}*Nb*	^{98}*Mo*	^{101}*Ru*	^{103}*Rh*	^{108}*Pd*	^{109}*Ag*	^{111}*Cd*	^{115}*In*
1	cps		3	1				9			2		2		357	19154912	1	
2	cps	6						21		4		3			355	24689529	2	2
1	ppm														2.73	92940		
2	ppm	0.06													2.72	119794		0.004

Laser ablation track	*Unit*	^{120}*Sn*	^{121}*Sb*	^{126}*Te*	^{133}*Cs*	^{138}*Ba*	^{139}*La*	^{140}*Ce*	^{141}*Pr*	^{145}*Nd*	^{151}*Eu*	^{157}*Gd*	^{159}*Tb*	^{162}*Dy*	^{165}*Ho*	^{167}*Er*	^{169}*Tm*	^{172}*Yb*
1	cps	12	598	5		2		1									1	
2	cps	31	1401	2	5	9	2	3	6	2				2				
1	ppm	0.05	2.33	0.08														
2	ppm	0.14	5.45	0.04														

Laser ablation track	*Unit*	^{175}*Lu*	^{178}*Hf*	^{181}*Ta*	^{182}*W*	^{185}*Re*	^{189}*Os*	^{193}*Ir*	^{195}*Pt*	^{202}*Hg*	^{205}*Tl*	^{208}*Pb*	^{209}*Bi*	^{232}*Th*	^{238}*U*
1	cps									84315		26	4		
2	cps					1				118857		14	4		
1	ppm									291		0.08	0.009		
2	ppm									410		0.04	0.007		

Notes: cps, count per second; ppm, parts per million

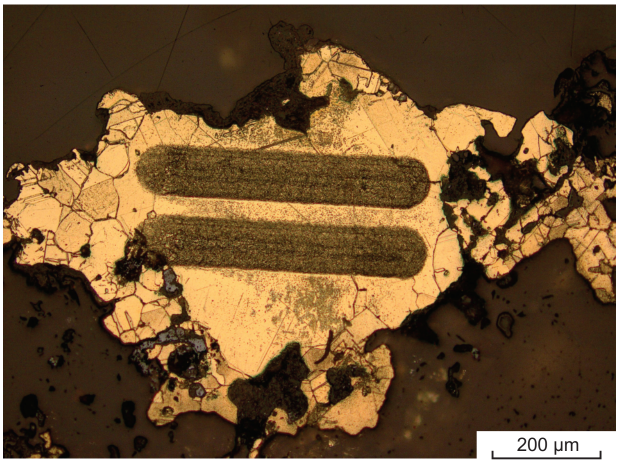

Figure 4. Reflected-light photomicrograph of gold microstructure, after aqua regia etching, from sample 201967: gold specks in quartz, Middle Creek prospect. Dark elongate lines are laser ablation tracks produced during LA-ICP-MS analyses

References

Bagas, L 2005, Geology of the Nullagine 1:100 000 sheet: Geological Survey of Western Australia, 1:100 000 Geological Series Explanatory Notes, 33p.

Ferguson, KM and Ruddock, I 2001, Mineral occurrences and exploration potential of the East Pilbara: Geological Survey of Western Australia, Report 81, 114p.

Geological Survey of Western Australia 2014, Pilbara, 2014: Geological Survey of Western Australia, Geological Information Series, data package.

Hancock, EA and Beardsmore, TJ 2020, Provenance fingerprinting of gold from the Kurnalpi Goldfield: Geological Survey of Western Australia, Report 212, 21p.

Hickman, AH 1983, Geology of the Pilbara Block and its environs: Geological Survey of Western Australia, Bulletin 127, 268p.

Hickman, AH 2021, East Pilbara Craton: a record of one billion years in the growth of Archean continental crust: Geological Survey of Western Australia, Report 143, 187p.

Hickman, AH 2022, Mosquito Creek Formation (A-NUq-mh): Geological Survey of Western Australia, WA Geology Online, Explanatory Notes extract, viewed 5 April 2022, <www.dmirs.wa.gov.au/ens>.

Murray, S 2009, LBMA certified reference materials. Gold project final update: The London Bullion Market Association, Alchemist, no. 55, p. 11–12.

Recommended reference for this publication

Hancock, EA, Blay, OA and Beardsmore, TJ 2022, 201967: gold specks in quartz, Middle Creek prospect; GSWA Mineralogy Record 1: Geological Survey of Western Australia, 5p.